Accelerated SubpiX – A CT Sub-pixel Super Resolution Technique

Lucas Determan[1], Kirk Busche[1], Pradeep Bhattad[1]

[1]North Star Imaging, Inc., Rogers, MN, United States of America, e-mail: ldeterman@4nsi.com, kbusche@4nsi.com, pbhattad@4nsi.com

Abstract
The resolution of standard CT scans is dictated by the physical constraints of the detector's sampling resolution. Super resolution is a class of techniques used to improve the reconstruction resolution beyond the physical limitations of the detector, via pure computational methods or with novel trajectories to acquire additional data. This work characterizes an improved accelerated super resolution technique that builds upon an existing method, SubpiX, and acquires projections along a trajectory of sub-pixel detector translations. The sub-pixel shifts introduce sampling across the spatial domain of each pixel, allowing the resulting images to be combined and upsampled to a higher resolution projection for reconstruction. This technique is shown to be flexible, allowing for different amounts of additional data to improve reconstruction quality at the cost of increased acquisition length. This paper compares the super resolution results using various amounts of additional acquired data.

Keywords: Super resolution, Computed Tomography, Reconstruction

1 Introduction

Spatial resolution is an important metric in non-destructive evaluation of parts using X-ray CT. The resulting resolution of the final reconstructed volume is limited by the detector's pixel pitch, which is a fixed physical property. Improving the sampling resolution of a detector is often not feasible as this requires constructing a different detector with smaller pixels, so algorithmic approaches are attractive alternatives. Super resolution refers to the algorithmic process of recovering high-resolution images from low-resolution images and has been studied across many domains [1] [2]. These techniques can generally be classified into two categories: single-image super resolution, where the high-resolution image is produced via computational post-processing from a single low-resolution image; and multiple-image super resolution, where the high-resolution image is produced by combining multiple low-resolution images acquired at sub-pixel shifts [2] [3] [4] [5]. Recent works have shown significant strides in improving single-image super resolution using deep learning [6] [7], however these successes have been difficult to apply to computed tomography (CT) due to a lack of high quality supervised datasets consisting of ground truth high-resolution images and corresponding low-resolution images. Multiple-image super resolution avoids the need for a large training corpus by synthesizing the high-resolution image directly from multiple real acquisitions sampled along sub-pixel shifts. However, multiple-image methods require more input samples acquired at precise translations to ensure a high-quality high-resolution image is recovered. In the simplest case, an upsampling factor of d (in both the vertical and horizontal directions) requires a minimum of d^2 low-resolution samples to recover the high-resolution image, leading to a d^2 increase in acquisition time.

In a CT reconstruction, the pixel pitch and scan magnification define the voxel size and therefore define the voxel resolution. This optimal voxel size for a reconstruction is given by pixel pitch divided by the scan magnification. Super resolution techniques enable a smaller voxel size by increasing the relative pixel density in the high-resolution image, while maintaining the same geometric magnification in the scan. A super resolution technique which upsamples the low-resolution images by a factor of d thus has an optimal voxel size proportionally scaled by $1/d$. This paper investigates the effects of reducing the number of low-resolution samples in conjunction with interpolation for super resolution and the resulting tomographic reconstructions using these high-resolution images.

2 Method

The super resolution problem can be modeled as a linear system relating the $\boldsymbol{k}$th observed low-resolution image $\boldsymbol{y_k}$ to the ideal high-resolution image $\boldsymbol{x}$ in the spatial domain via

$$\boldsymbol{y_k} = \boldsymbol{A_k x} + \boldsymbol{n_k} \tag{1}$$

where $\boldsymbol{A_k}$ is the projection dependent system matrix and $\boldsymbol{n_k}$ is additive noise [1] [2]. The system matrix $\boldsymbol{A_k}$ is generally assumed to be composed of a downsampling operator $\boldsymbol{D}$, a blurring operator $\boldsymbol{B_k}$, and a motion and warping operator $\boldsymbol{M_k}$

$$\boldsymbol{A_k} = \boldsymbol{D B_k M_k}. \tag{2}$$

In X-ray CT with known system geometry, the low-resolution samples for the same projection angle θ can be approximated with a shared blurring model $\boldsymbol{B} = \boldsymbol{B_k}$ (e.g. Gaussian blur), and the motion operator is simply the known detector translations for each low-resolution sample position.

One method for recovering $\boldsymbol{x}$ is SubpiX, a super resolution technique employed at North Star Imaging (NSI) which uses precise sub-pixel motion of the X-ray system to fuse into high-resolution images [5]. Let the sub-pixel translations of the detector (x, y) be defined as the set

$$T_d: \left\{(x,y): \left\{x: i * \frac{p_x}{d}, \ \ \forall i \in [0,d)\right\} \cup \left\{y: j * \frac{p_y}{d}, \ \ \forall j \ \in [0,d)\right\}\right\} \tag{3}$$

where p_x and p_y are the low-resolution image pixel pitch in the horizontal and vertical directions respectively. Note T_d contains d^2 unique translations, e.g. for an upsampling factor $d = 2$, $T_2 = \{(0,0), \left(\frac{p_x}{2}, 0\right), \left(\frac{p_x}{2}, \frac{p_y}{2}\right), \left(0, \frac{p_y}{2}\right)\}$, so a unique index k can be assigned to each translation combination. A pixel of the high-resolution image, $x_{i,j}$ is constructed from the pixels of $y_{k,u,v}$, $\forall k \in [0, d^2)$ such that the low-resolution pixels lie within a spatial neighborhood (U_i, V_j) of the sample location of $x_{i,j}$

$$\boldsymbol{x}_{i,j} = f_{\{(u,v)\in(U_i,V_i)\}}(\boldsymbol{y}_{k,u,v}), \qquad \forall k \in [0, d^2). \tag{4}$$

The existing SubpiX method requires d^2 low-resolution images for recovery of the high-resolution image in addition to a known system model. The low-resolution images are acquired by precisely translating the detector vertically and horizontally along a grid with uniform sub-pixel spacing, e.g. 0.5-pixel spacing for an upsampling factor of $d = 2$. In practice, the increase in spatial resolution has diminishing returns as $d > 2$ particularly with the increase of acquisition time increasing by d^2, so the typical SubpiX acquisition consists of 4 Tiles for an upsampling factor of 2. This procedure is repeated for each projection angle θ, with the resulting high-resolution images used to reconstruct a high-resolution volume via filtered backprojection.

Accelerated SubpiX improves upon SubpiX by reducing the number of lower resolution images needed to produce a high-resolution image, thus reducing the acquisition time and data footprint. Since each single low-resolution pixel samples across multiple high-resolution pixels, the number of low-resolution samples needed to produce a high-resolution image can be reduced. For an upsampling factor of $d = 2$, two methods are proposed: 2 Tile and 1 Tile Accelerated SubpiX. In the 2 Tile mode, only two of the low-resolution images (tiles) are acquired for each projection

$$\boldsymbol{x}_{i,j} = f_{2,\{(u,v)\in(U_i,V_i)\}}(\boldsymbol{y}_{k,u,v}), \qquad \forall k \in C(d^2, 2). \tag{5}$$

To compensate for the reduction in sub-pixel samples, $\boldsymbol{f_2}(\cdot)$ is modified from the original SubpiX method (3) with additional interpolation. Compared to the 4 Tile method, this 2 Tile method results in a two-fold decrease in acquisition time and low-resolution images acquired. A similar technique is used for the 1 Tile mode a single low-resolution image is used to recover the high-resolution image

$$\boldsymbol{x}_{i,j} = f_{1,\{(u,v)\in(U_i,V_i)\}}(\boldsymbol{y}_{k,u,v}), \qquad k \in C(d^2, 1). \tag{6}$$

As with the original SubpiX, the resultant high-resolution images are recovered for each angular position of the CT scan and reconstructed into a high-resolution volume using filtered backprojection.

3 Experiment Setup

Several experiments were conducted to measure the performance of the proposed super resolution techniques. The experiments consisted of scanning several objects including a piston rod, cellphone, aluminum cylinder, and lollipop candy. These objects were selected to characterize the performance of Accelerated SubpiX on various feature sizes, material, and system specifications. Each object was scanned a total of three times: (1) along the original (4 Tile) SubpiX trajectory, (2) along an accelerated trajectory acquiring two low-resolution images for each angular position, and (3) along an accelerated trajectory acquiring a single low-resolution image for each angular position. The acquisition parameters used for each scan is listed in Table 1.

Table 1: Acquisition parameters.

Object	*Source*	*Voltage [kV]*	*Current [μA]*	*Pixel Pitch [μm]*	*FPS*	*Frame Averaging*	*Magnification*
Piston Rod	Microfocus	210	400	127	12.5	10	1.48x
Phone	Microfocus	225	80	300	6	3	8.82x
1695 Cylinder	Microfocus	210	30	127	5	10	12.58x
Candy	Microfocus	100	330	300	28.04	10	1.48x

In total, four reconstructions were generated for each part: standard low resolution, 1 Tile Accelerated SubpiX, 2 Tile Accelerated SubpiX, and 4 Tile SubpiX. Each reconstruction for a given part uses similar system geometry and volume

definitions, allowing for easy voxel comparisons. The standard circular reconstruction was done using data from a single low-resolution tile of the 4 Tile SubpiX acquisition, however this low-resolution scan was reconstructed into a voxel grid with the same voxel size as the super resolution techniques. This ensures a fair comparison and confirms the improvement in the spatial resolution is not simply from reconstructing into a high-resolution volume. The super resolution techniques were then reconstructed into the same high-resolution volume definition. To validate the reduction in acquisition time, a unique scan for each technique was also acquired.

A trade-off study was conducted to evaluate the performance of each mode given acquisition time, data size, and reconstruction quality. The reconstruction quality was compared by inspecting slices from each volume, comparing against the baseline low-resolution scan and the original SubpiX scan. In addition to the qualitative comparison of the objects, an aluminum cylinder was also scanned in accordance with the ASTM E1695 standard. This industry standard outlines a method for measuring the spatial resolution and contrast discrimination of a CT system and scan [8].

4 Results

The first object was a piston rod made from cast aluminum. As a casting, many small features such as porosities and cracks are visible and demonstrate the capabilities of the various modes considered. Figure 1 shows slices of the piston rod from the baseline standard low-resolution reconstruction and each super resolution method mode. Note the improved edge resolution of the small features from all three super resolution techniques relative to the standard CT method as expected. With the largest amount of data used to produce the super resolution images, the 4 Tile is expected to show the maximum enhancement. On this sample, the 2 Tile super resolution method approaches the 4 Tile resolution enhancement, but with half of the low-resolution sample data. The 1 Tile shows a resolution improvement over the standard CT scan, but the reduction in sample data is apparent compared to the other super resolution methods, in part with the increase in noise present.

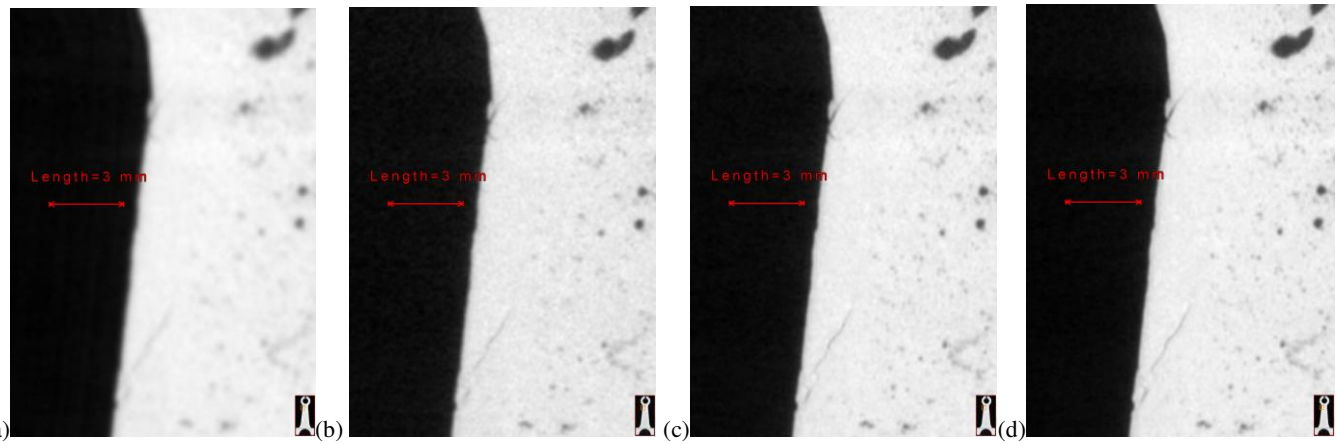

(a) (b) (c) (d)

Figure 1: Slice of piston rod reconstruction from (a) Standard CT, (b) 1 Tile, (c) 2 Tile, (d) 4 Tile.

The next object considered was a cellphone as modern electronics contain many small features which benefit from high-resolution scanning. Figure 2 shows a comparison of a slice through the battery of the cellphone reconstructed using each method. The two reduced-data methods proposed show similar performance to the 4 Tile SubpiX, with enhanced resolution compared to the standard circular reconstruction. As before, the reconstruction quality improves as more data is used to reconstruct. The 1 Tile SubpiX reconstruction shows significant improvements over the standard circular reconstruction with the same amount of projections acquired. However, it again shows that acquiring more low-resolution samples (2 Tile, 4 Tile) help suppress the noise present in the low-resolution radiographs.

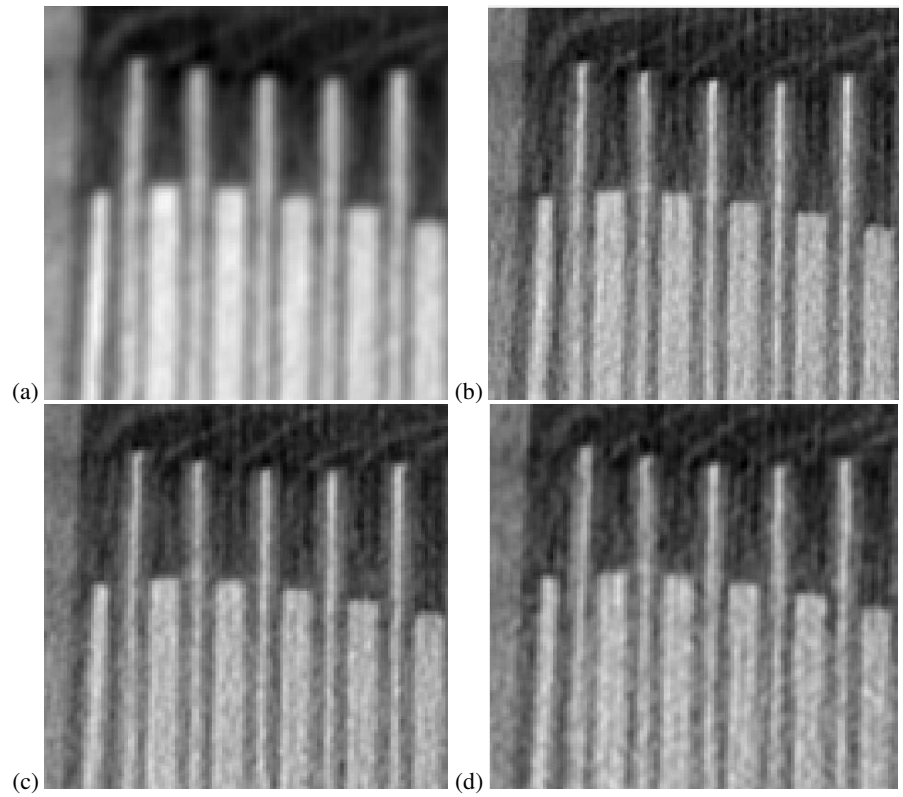

Figure 2: Slice of cellphone battery from (a) standard circular scan, (b) 4 Tile SubpiX, (c) 2 Tile SubpiX, and (d) 1 Tile SubpiX.

In another slice of the phone, shown in Figure 3, the circuitry can be observed with one of the microprocessors and its contact points. The comparison between the standard CT scan with 1 Tile SubpiX shows significant improvement can be made in the quality of the scan with the same amount of data by using the proposed super resolution technique.

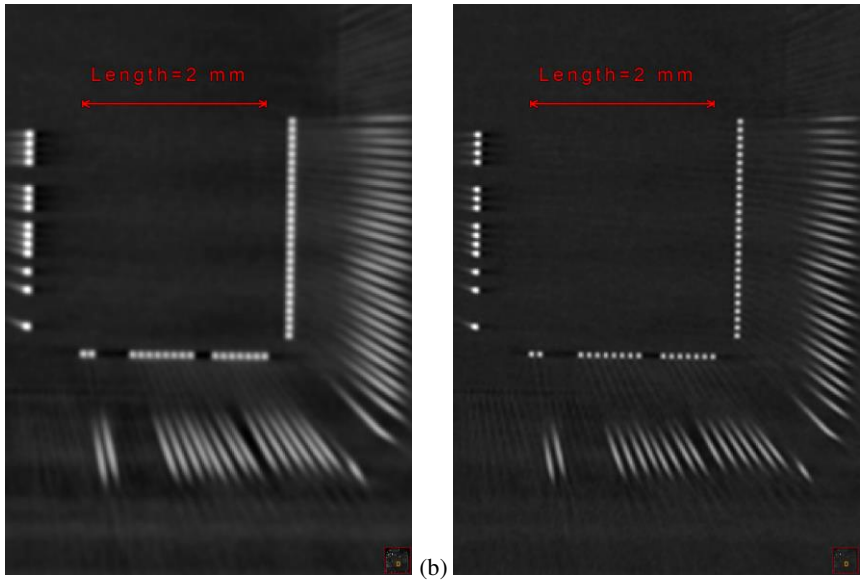

Figure 3: Slice of the phone showing a microprocessor and contact points in (a) a standard CT scan and (b) 1 Tile SubpiX.

The final qualitative object considered was the candy lollipop shown in Figure 4. The voids in the candy and the tightly wound paper stick provide small features to contrast the performances of each method. As expected, the 4 Tile SubpiX produces the highest quality scan while the standard scan is the lowest. The 1 Tile again shows an increased sensitivity to noise; however, it continues to produce a high-resolution scan. As with the previous scans, the 2 Tile method shows a similar performance to 4 Tile SubpiX, with a balance of enhanced resolution performance and minimal additional noise influence.

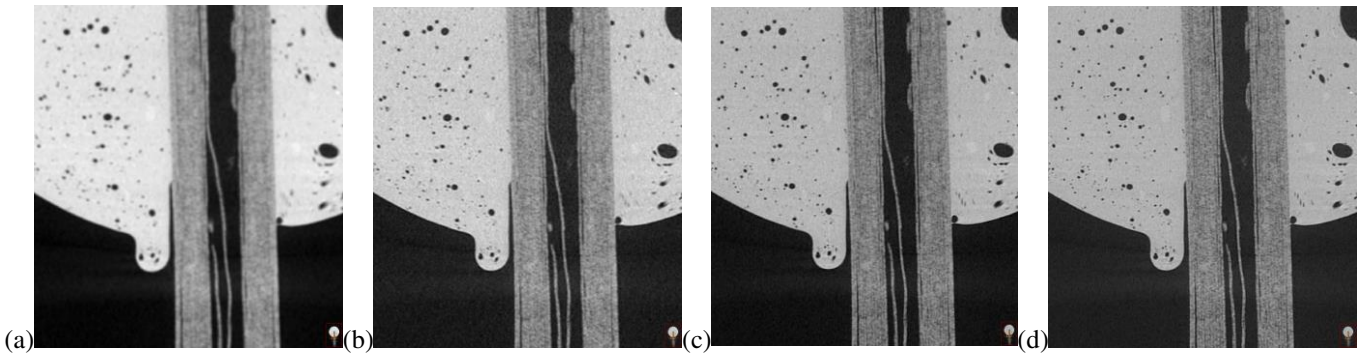

Figure 4: All the X slices of the candy lollipop (a) standard CT, (b) 1 Tile, (c) 2 Tile, and (d) 4 Tile.

To quantitatively assess resolution enhancement and scan quality, an ASTM E1695 analysis was performed on a scan of a solid aluminum cylinder. The standard outlines a procedure for measuring the spatial resolution, contrast sensitivity, and contrast to noise ratio (CNR) of a CT reconstruction [8]. The analysis was performed on the standard circular, 1 Tile, 2 Tile, and 4 Tile SubpiX scans. Each of the SubpiX variations show spatial resolution improvement over the standard circular scan in Figure 5. The analysis also shows spatial resolution continues to improve as more low-resolution samples are used. CNR also improves as additional data is used across super resolution techniques. However, the standard circular scan has significantly better CNR than all the SubpiX reconstructions which can be attributed to the super resolution process enhancing high frequency components, such as edges and noise.

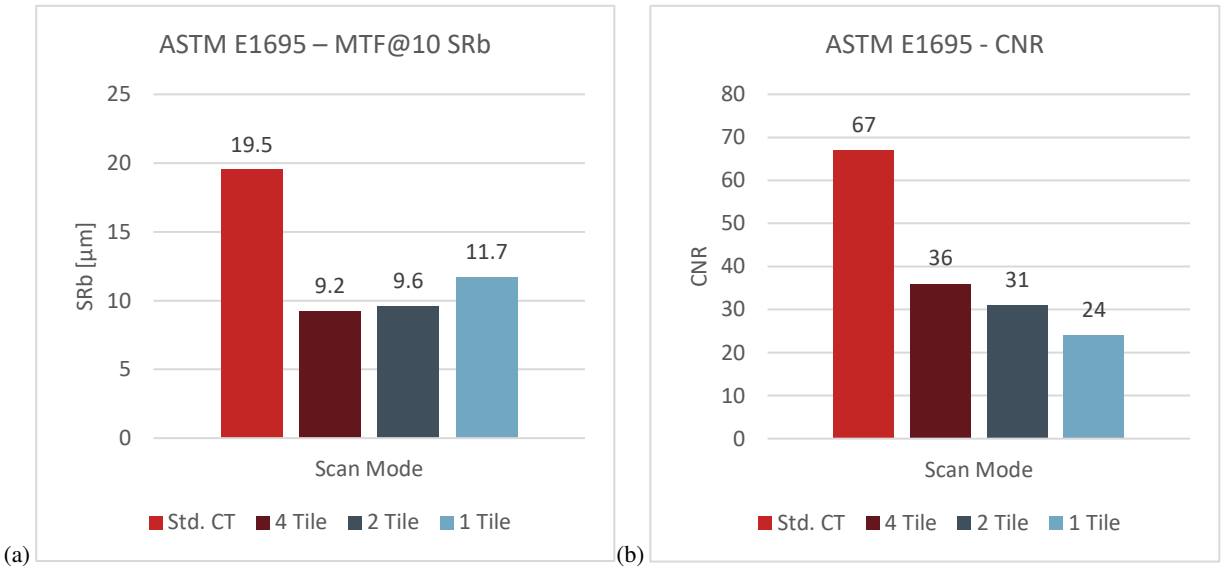

Figure 5: ASTM E1695 results showing (a) spatial resolution and (b) contrast to noise results.

These analyses show the quality of the 1 Tile and 2 Tile scans were similar but not equivalent to the 4 Tile SubpiX. However, both proposed super resolution techniques showed significant spatial resolution improvement compared to standard circular scan, but were achieved with a fraction of the 4 tile SubpiX acquisition time. As expected, the reduction in necessary low-resolution images led to a proportional decrease in acquisition time across the proposed methods, shown in Figure 6. For both the phone and candy lollipop objects, a unique standard circular scan was not collected, therefore no data is provided for timing. However, it is expected that the standard low-resolution scan would have an acquisition time equivalent to the 1 Tile SubpiX acquisition, as seen with the piston rod and aluminum cylinder. In addition to a reduction in acquisition time, the file storage footprint is also proportional to the number of low-resolution images required, as the super resolution recovery is performed at the time of reconstruction, to avoid storing the large file sizes of the high-resolution images.

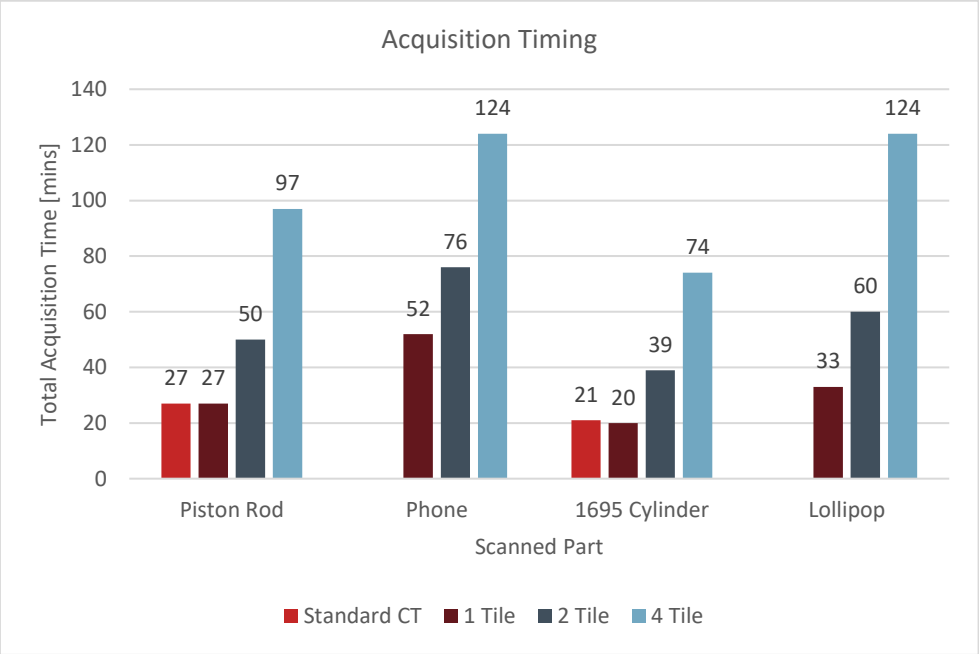

Figure 6: Total acquisition time for each scanned part.

5 Conclusion

In this paper, the number of low-resolution images needed for multiple-image super resolution was analyzed to enable enhanced volume resolution with reduced acquisition time. Acquisition time is an important consideration for industrial NDT as it dictates throughput and affects the CT system's cycle time. The analysis of the proposed methods show resolution enhancement can be achieved with a fraction of the data when compared to existing multiple-image super resolution techniques. Using ASTM E1695, the spatial resolution showed comparable enhancement with each of the 4 Tile, 2 Tile, and 1 Tile modes. The reduction in low-resolution data led to a decrease in contrast-to-noise in the ASTM E1695 results, which was attributed to the lack of redundant data to remove the effects of noise in addition to the super resolution technique enhancing high-frequency components. In addition to enhancing resolution with increased acquisition speed, the proposed methods also reduce the effective radiograph file storage footprint by acquiring less data while creating the high-resolution image on-the-fly during reconstruction. For industries where data is retained for long periods, this method can result in less overall necessary storage capacity. Overall, the introduced Accelerated SubpiX and its two new modes suggest that super resolution can be achieved with the same level of data as a standard CT scan. Future work will focus on developing methods for recovering a high-resolution image with limited low-resolution samples that further improve spatial resolution and contrast-to-noise performance.

References

[1] S. C. Park, M. K. Park and M. G. Kang, "Super-resolution image reconstruction: a technical overview," *IEEE Signal Processing Magazine,* vol. 20, pp. 21-36, 2003.

[2] K. Nasrollahi and T. B. Moeslund, "Super-resolution: a comprehensive survey," *Machine Vision and Applications,* vol. 25, p. 1423–1468, 2014.

[3] K. Sun, S. Kieß and S. Sven, "Spatial resolution enhancement based on detector displacement for computed tomography," in *Proc. Conf. Industrial Computed Tomography*, 2019.

[4] K. Sun, T.-H. Tran, J. Guhathakurta and S. Simon, "FL-MISR: fast large-scale multi-image super-resolution for computed tomography based on multi-GPU acceleration," *Journal of Real-Time Image Processing,* vol. 19, p. 331–344, 2022.

[5] Y. Wang, J. A. Sharpe, J. Schlecht, E. Ferley and J. Noel, "High-resolution computed tomography". United States of America Patent US20160047759A1, 4 October 2016.

[6] W. Yang, X. Zhang, Y. Tian, W. Wang, J.-H. Xue and Q. Liao, "Deep Learning for Single Image Super-Resolution: A Brief Review," *Trans. Multi.,* vol. 21, p. 3106–3121, December 2019.

[7] J. Park, D. Hwang, K. Y. Kim, S. K. Kang, Y. K. Kim and J. S. Lee, "Computed tomography super-resolution using deep convolutional neural network," *Physics in Medicine & Biology,* vol. 63, p. 145011, July 2018.

[8] *ASTM E1695 - 20e1, Standard Test Method for Measurement of Computed Tomography (CT) System Performance,* West Conshohocken: ASTM International, 2020.